Hindawi
Wireless Communications and Mobile Computing
Volume 2022, Article ID 8614952, 14 pages
https://doi.org/10.1155/2022/8614952

Research Article

Identification of Shortwave Radio Communication Behavior Based on Autocorrelation Spectrogram Features

Haitao Li,[1] **Xiang Chen**,[1] **Yingke Lei**,[1] **Pengcheng Li**,[1] **and Caiyi Lou**[2]

[1]*College of Electronic Countermeasures, National University of Defense Technology, Hefei 230037, China*
[2]*36th Research Institute of China Electronics Technology Group Corporation, Jiaxing 314033, China*

Correspondence should be addressed to Caiyi Lou; loucaiyi@126.com

Received 13 May 2022; Revised 25 August 2022; Accepted 29 August 2022; Published 22 September 2022

Academic Editor: Mingqian Liu

Cognitive communication behavior is becoming a research hotspot in the field of communication confrontation. In theory, the behavioral intention of noncooperating parties can be obtained by analyzing communication signals. Considering the complexity of the actual electromagnetic environment, even when the signal-to-noise ratio (SNR) is low, a certain accuracy still needs to be guaranteed. In this paper, according to five types of physical burst waveforms defined by the shortwave radio interoperability standard, a signal feature extraction method based on autocorrelation spectrogram features is proposed, and a two-input convolutional neural network (CNN) for classification is designed to improve the identification ability of shortwave communication behavior. The experimental results illustrate that the five kinds of shortwave radio communication behaviors can be accurately identified even when the noise is large. The research in this paper can directly analyze the communication behavior through physical layer signal without demodulation, which has the ability to grasp the communication behavior of the shortwave radio station in real time.

1. Introduction

Behavior is the active response of an organism such as a person or an animal to the internal and external environment under the control of thought. Research on behavior recognition based on machine learning (ML) [1–3] and probabilistic methods [4–7] has been developing rapidly. In recent years, the proposal of cognitive electronic warfare (CEW) requires that communication countermeasures be intelligent, and the concept of cognition has begun to receive attention in the field of communication. Research on cognitive radio [8], cognitive radar [9], cognitive Internet of Things (IoT) [10], and cognitive electronic jamming [11] has developed rapidly. Cognitive communication behavior is a potentially hot area. In electronic warfare, if enemy behaviors can be analyzed in real time, we can take actions in a timely manner, which is conducive to gaining advantages.

In 2010, a project called Behavioral Learning for Adaptive Electronic Warfare (BLADE) [12] was proposed to meet the needs of intelligent electromagnetic spectrum operations. The importance of behavioral learning was emphasized in the field of electronic warfare for the first time. It is meaningful to carry out behavioral recognition research based on wireless signals from communication radiation sources (CRSs). CRS itself is a concept without biological characteristics, but because of human operation, it has observable behavioral information that reflects the behavior of the operator. Taking a radio station as an example, its operator will perform operations such as calling, data transmission, image transmission, and switching on and off. The radio station will change its working mode and send different signals according to what the operator does; therefore, it has observable behavioral information. By analyzing the wireless signals obtained by reconnaissance, a series of behavioral information can be unscrambled, and the operator's task, situation, status, and other key information can be understood.

In recent years, machine learning (ML) has been applied in the field of signal processing, including signal modulation pattern recognition [13–16], CRS individual recognition [17–19], communication specific signal type recognition [20, 21], and other fields, and a series of achievements have

been achieved. However, research on CRS behavior recognition is still in the beginning stage. There have been very few relevant studies in the published literature thus far.

Research on communication behavior can be divided into communication group behavior [22, 23] and communication individual behavior [24–36]. The former mainly refers to a series of combat tasks coordinated by groups equipped with CRS, while the latter mainly refers to the working modes, tasks of a certain CRS, and the actions of the person or unit operating the CRS. Individual communication behavior is the focus of our research. At present, relevant research is mainly based on the following three methods. The first method is data mining for spectrum monitoring data to gain communication relationships [24–29]. The second method is to obtain the communication behavior by parsing the communication protocol. [30, 31]. The third method transforms the problem of communication behavior recognition into the problem of radio signal classification recognition by analyzing the behavior connotation of intercepted radio signals [32–36]. Liu et al. proposed a method to discover the communication relationship of ultrashort-wave radio stations [24]. In the literature [25], DBSCAN is improved and used to mine the hidden communication behavior of spectrum data. By mining the physical characteristics of the spectrum monitoring signal and analyzing their statistical laws, individual communication behavior can be known [26]. Mining of communication relations in the case of missing and disordered data is realized in the literature [27]. Pan et al. proposed a communication behavior structure mining algorithm, which can be used without analyzing the signal content to obtain the communication relation and the communication node of the target field communication [28]. Cheng et al. proposed a method called DECBR, which DCGAN was used for data enhancement and realized the identification of communication behaviors under small sample conditions [29]. Zhang et al. obtained the behavioral intention of the frequency hopping transmitter by analyzing the TDMA protocol [30]. You and Ge proposed a regular expression-based Fetion communication message identification method through the analysis of specific fields in the Fetion protocol, so as to achieve the purpose of inferring the Fetion communication behavior [31]. Zhou et al. observed the differences in the deep-level features of shortwave burst waveforms and demonstrated the feasibility of directly identifying shortwave communication behaviors based on physical layer signals [32]. Wu et al. used the improved LeNet to identify five communication behaviors [33]. Wu et al. [34] used the improved one-dimensional DenseNet to identify seven automatic link establishment (ALE) behaviors under the same types of burst waveform BW0. Furthermore, literature [35] conducted visualization research of the seven ALE behaviors mentioned in literature [34] and observed the deep-level feature differences of the seven ALE signals. Based on this, ACGAN was used to recognize seven types of ALE behavior under small sample conditions [36].

In this paper, the relationship between burst waveforms and communication behaviors is first introduced according to the five types of burst waveforms specified by the MIL-STD-188-141B standard, and then a feature extraction method is proposed for extracting the features of the autocorrelation spectrogram of the signal. The features extracted by this method are not easily polluted by noise, especially under the condition of low SNR, and more original features of the signal can be presented on the spectrogram. The main contributions of this paper are as follows:

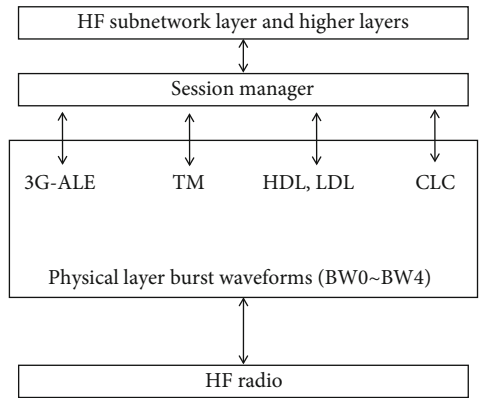

Figure 1: 3G HF protocol suite.

(i) we use the autocorrelation method to preprocess the signal and convert the noise-containing signal into an autocorrelation time series. This method is simple to calculate, can effectively reduce the interference of Gaussian white noise, and can facilitate subsequent feature extraction

(ii) we perform bispectral transformation on the autocorrelation time series and extract bispectral features. The higher-order spectral domain can present some feature differences that cannot be presented in the time domain. It is convenient to save the extracted features in a format similar to a picture, which is beneficial to the processing of the CNN. Compared with traditional method, this method can significantly improve the recognition accuracy under low SNR conditions

(iii) we design a two-input CNN for classification recognition. The extracted autocorrelation spectral features are input into the two branches of the neural network, and then the outputs of the two branches are processed. This two-input CNN can further extract features and reduce the possibility of incorrect decisions, meanwhile, it does not require much additional computing time

2. Background

The third-generation shortwave communication protocol standard MIL-STD-188-141B is proposed to develop adaptive short-wave communication, realize shortwave link establishment, link maintenance, shortwave network construction, and improve communication quality. Corresponding burst waveforms are defined in this standard for the various kinds of signaling required in the short-wave

Wave form	Used for	Burst duration	Payload	Preamble	FEC coding	Inter-leaving	Data format	Effective code rate
BW0	3G-ALE PDUs	613.33ms 1472 PSK symbols	26 bits	160.00 ms 384 PSK symbols	Rate = 1/2, K = 7 convolutional (No flush bits)	4 × 13 block	16-ary orthogonal walsh function	1/96
BW1	Traffic management PDUs, HDL acknowledgement PDUs	1.30667 seconds 3136 PSK symbols	48 bits	240.00 ms 576 PSK symbols	Rate = 1/3, K = 9 convolutional (No flush bits)	16 × 9 block	16-ary orthogonal walsh function	1/144
BW2	HDL traffic data PDUs	640 + (n*400) ms 1536 + (n*960) PSK symbols n = 3, 6, 12, or 24	n*1881 bits	26.67 ms 64 PSK symbols (for equalizer training)	Rate = 1/4, K = 8 convolutional' (7 flush bits)	None	32 unknown/ 16 known	Variable 1/1 to 1/4
BW3	LDL traffic data PDUs	373.33 + (n*13.33) ms 32n + 896 PSK symbols, n = 64, 128, 256 or 512	8n + 25 bits	266.67 ms 640 PSK symbols	Rate = 1/2, K = 7 convolutional' (7 flush bits)	24 × 24, 32 × 3444 × 48, or 64 × 65 convolutional block	16-ary orthogonal walsh function	Variable 1/12 to 1/24
BW4	LDL acknowledgement PDUs	640.00 ms 1536 PSK symbols	2 bits	None	None	None	4-ary orthogonal walsh function	1/1920

Figure 2: Details of different burst waveforms.

communication system, to meet distinctive requirements for payload, duration, time synchronization, acquisition, and demodulation performance in the presence of noise, fading, and multipath. Figure 1 shows its basic architecture.

Among them, the physical layer defines five burst waveforms to perform different tasks, including BW0, BW1, BW2, BW3, and BW4. In Figure 2, the details of the five types of burst waveforms are summarized, which contain signal parameters, application scenarios, and other information.

Further, the generation process of the five burst waveforms is shown in Figure 3.

Each type of burst waveform can achieve its own function in short-wave communication. BW0 is used for third-generation automatic link establishment (3G ALE), BW1 is used for traffic management (TM), BW2 and BW3 are used for data transmission, respectively, high-rate data link (HDL) and low-rate data link (LDL) transmission, and BW4 is used for LDL acknowledgment. To clarify what these behaviors are, we will explain them one by one.

ALE encompasses establishing a communication link for shortwave communication. TM represents coordinating traffic exchanges on connections established based on the 3G-ALE protocol, and establishing a traffic link on which traffic can be delivered. HDL consists of providing reliable high-rate point-to-point data transfer service over the established links, while LDL means providing reliable low-rate point-to-point data transfer service.

This also illustrates that different burst waveforms correspond to different communication behaviors, which is summarized in Table 1.

3. Methods

Figure 4 shows the simple technical route of our research. On the basis of the burst waveforms of the physical layer, we carry out research on the identification of the communication behavior of the shortwave radio. Since behavior is a concept that describes biology, it is necessary to explain its meaning in the field of communication. Then, the mapping relationship between communication behaviors and burst waveforms needs to be found; both steps are mentioned in the second section. After the previous steps, the problem is transformed into the problem of signal processing and classification. In this section, the method of signal preprocessing is given, while the structure of the network model is designed.

3.1. Signal Denoising by the Autocorrelation Method. Suppose $x(t)$ is a random signal, R_{xx} is the autocorrelation function of $x(t)$, which is defined as the degree of correlation of $x(t)$ at different times. Then the definition formula of R_{xx} is as follows:

$$R_{xx}(\tau) = E\{x(t+\tau)x(t)\} \tag{1}$$

Therefore, assume $n(t)$ is the additive white Gaussian noise (AWGN), its mean is 0 and its variance is δ_n^2, $x(t)$ is the transmitter signal, $n(t)$ and $x(t)$ are uncorrelated, and $s(t)$ is the receiver signal, that is,

$$s(t) = x(t) + n(t). \tag{2}$$

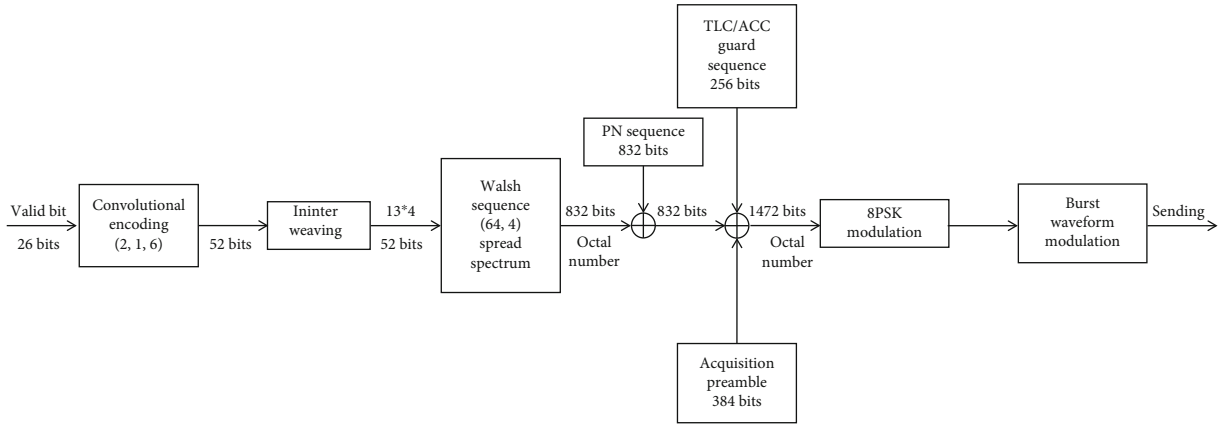

(a) The generation process of BW0

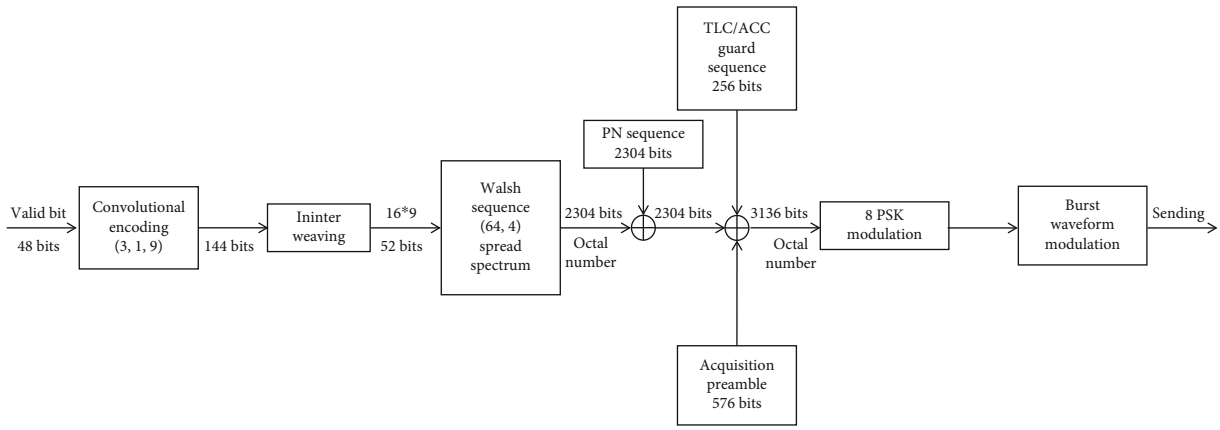

(b) The generation process of BW1

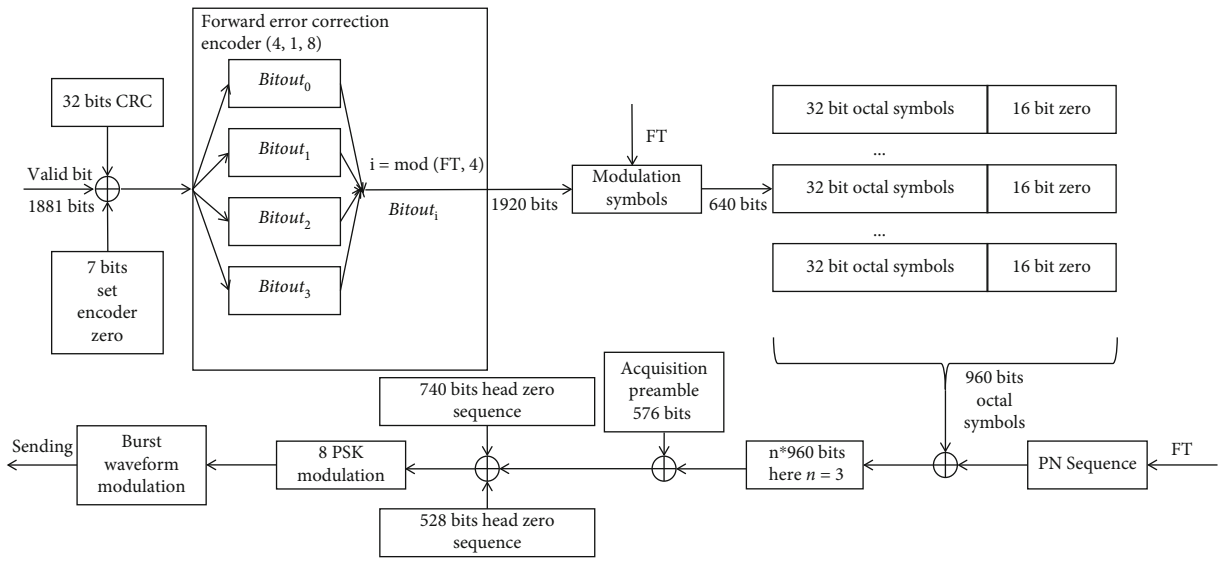

(c) The generation process of BW2

Figure 3: Continued.

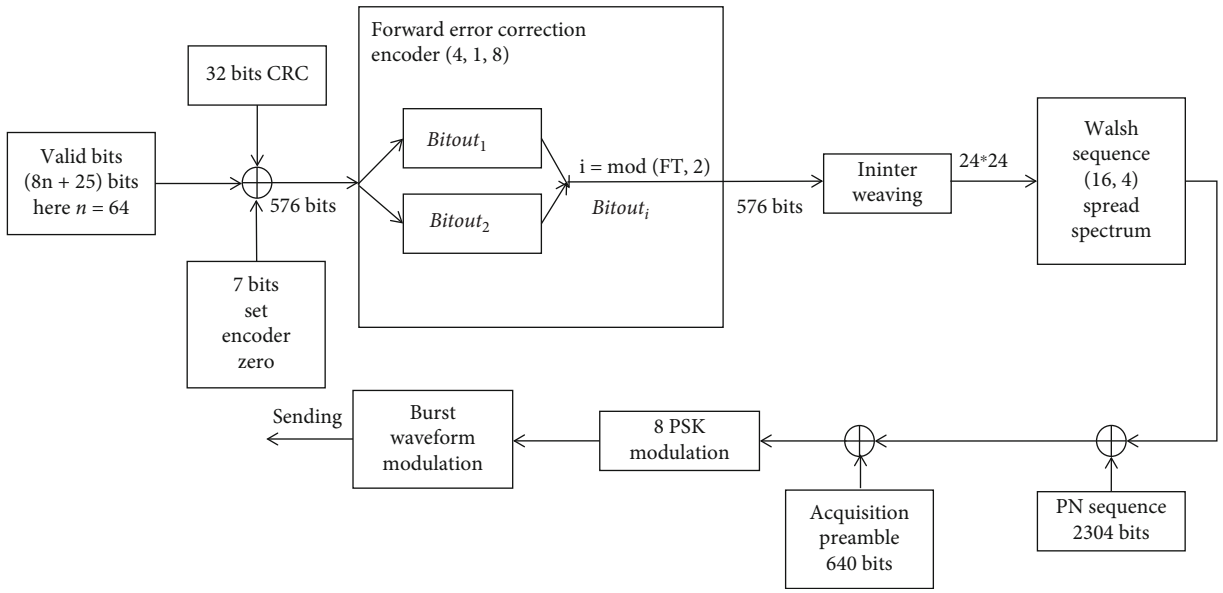

(d) The generation process of BW3

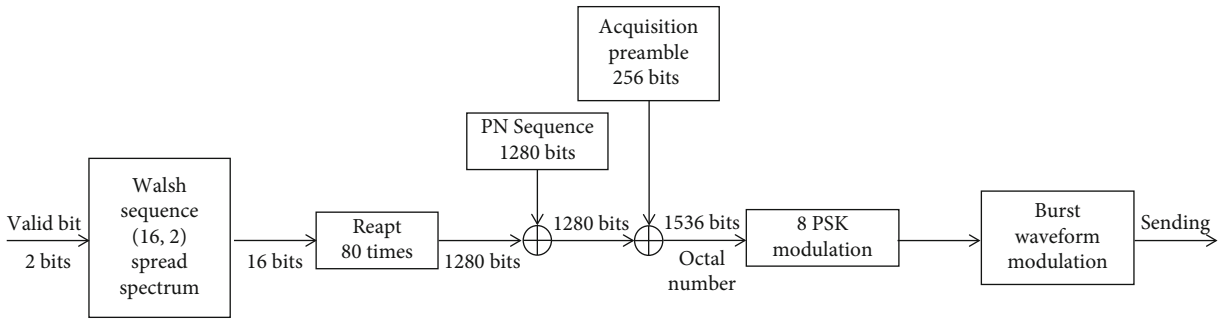

(e) The generation process of BW4

Figure 3: Signal generation process of burst waveforms.

Table 1: The connection between burst waveforms and behaviors.

Physical layer signal	Behavioral meaning
BW0 burst waveform	Automatic link establishment
BW1 burst waveform	Traffic management and HDL acknowledgment
BW2 burst waveform	Transfers of traffic data by the HDL protocol
BW3 burst waveform	Transfers of traffic data by the LDL protocol
BW4 burst waveform	LDL acknowledgment

Then, according to Equation (1), the autocorrelation function of $s(t)$ can be expressed as

$$R_{ss}(\tau) = E\{s(t+\tau)(s(t)\} = E\{(x(t+\tau) + n(t+\tau))(x(t) + n(t))\} = R_{xx}(\tau) + R_{xn}(\tau) + R_{nx}(\tau) + R_{nn}(\tau) = R_{xx}(\tau) + R_{nn}(\tau). \quad (3)$$

Since $n(t)$ has the following nature

$$R_{nn}(\tau) = E\{n(t+\tau)(n(t)\} = \begin{cases} 0, & \tau \neq 0, \\ \delta_n^2, & \tau = 0. \end{cases} \quad (4)$$

Then, (Equation (3)) can be converted to (Equation (5))

$$R_{ss}(\tau) = \begin{cases} R_{xx}(\tau), & \tau \neq 0, \\ R_{xx}(\tau) + \delta_n^2, & \tau = 0. \end{cases} \quad (5)$$

where τ is the time difference, which can take positive or negative numbers.

Therefore, it is proven that the autocorrelation function of $s(t)$ is not easily affected by AWGN. When the SNR is 0 dB, the time domain waveform of BW0 is shown in Figure 5. The abscissa represents the duration of the signal, and the ordinate represents the amplitude of the signal.

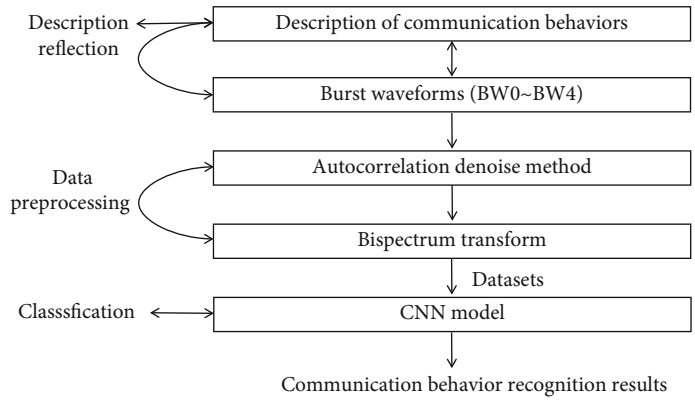

Figure 4: Simple technical route.

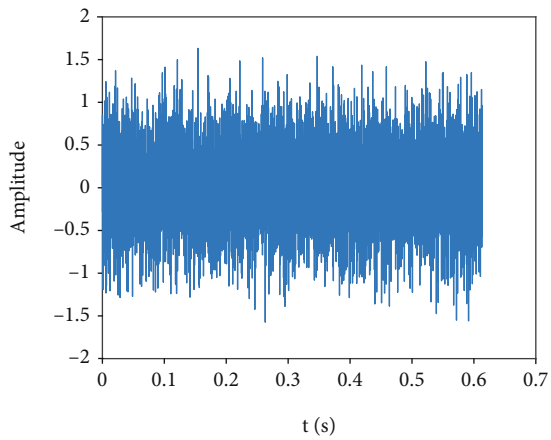

Figure 5: BW0 time domain signal (SNR = 0 dB).

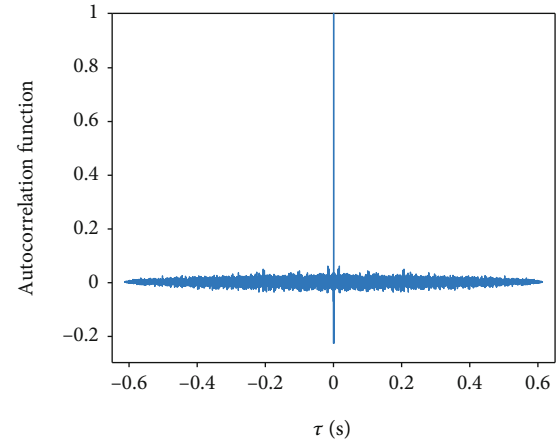

Figure 6: Autocorrelation function of BW0 (SNR = 0 dB).

According to Equation (5), the autocorrelation denoising curve of BW0 is shown in Figure 6. The abscissa is the time difference, and the ordinate is the autocorrelation function.

3.2. High-Order Spectral Analysis of Signals. Compared with the power spectrum, the higher-order spectrum contains more useful information, therefore, it can be considered as the development of the power spectrum. The bispectrum of the signal, also called the third-order spectrum, is the most basic higher-order spectrum. It has the advantages of requiring a small amount of calculation, suppressing AWGN to a certain extent [37], and retaining the original information of the signal as much as possible, so it is widely used in the field of signal processing.

The bispectrum S_{3x} and third-order cumulant c_{3x} of $x(t)$ are defined as follows:

$$S_{3x}(\omega_1, \omega_2) = \sum_{\tau_1=-\infty}^{\infty} \sum_{\tau_2=-\infty}^{\infty} c_{3x}(\tau_1, \tau_2) e^{-j(\omega_1\tau_1+\omega_2\tau_2)}, \tag{6}$$

$$\begin{aligned} c_{3x}(\tau_1, \tau_2) &= E[x(t)x(t+\tau_1)x(t+\tau_2)] - E[x(t)]E[x(t+\tau_1)x(t+\tau_2)] \\ &\quad - E[x(t+\tau_1)]E[x(t)x(t+\tau_2)] - E[x(t+\tau_2)]E[x(t)x(t+\tau_1)] \\ &\quad + 2E[x(t)]E[x(t+\tau_1)]E[x(t+\tau_2)] = cum[x(t)x(t+\tau_1)x(t+\tau_2)]. \end{aligned} \tag{7}$$

Among them, the necessary and sufficient condition for the existence of S_{3x} is that the third-order cumulant c_{3x} is absolutely summable, that is,

$$\sum_{\tau_1=-\infty}^{\infty} \sum_{\tau_2=-\infty}^{\infty} |c_{3x}(\tau_1, \tau_2)| < \infty, \tag{8}$$

where τ_1 and τ_2 are independent variables of c_{3x}, representing two time differences, ω_1 and ω_2 are the axes of the bispectral two-dimensional plane [38]. Through bispectrum transformation, the signal is transformed from the time domain to the spatial domain, which can retain more useful information.

3.3. Feature Extraction Process. The autocorrelation spectrum of the signal $s(t)$ can be calculated according to Equations (5), (6), and (7), and the specific process is as follows:

(a) According to Equation (5), calculate the autocorrelation function R_{ss} of $s(t)$.

(b) Calculate the third-order cumulant c_{3s} of R_{ss}, and then calculate the bispectrum S_{3x} of R_{ss} according to Equation (7). Here, we denote S_{3x} as the autocorrelation spectrum of $s(t)$.

When the SNR is 0 dB, we plot the autocorrelation spectrogram pictures of five kinds of burst waveforms, as shown in Figure 7, where f_1 and f_2 are normalized frequencies.

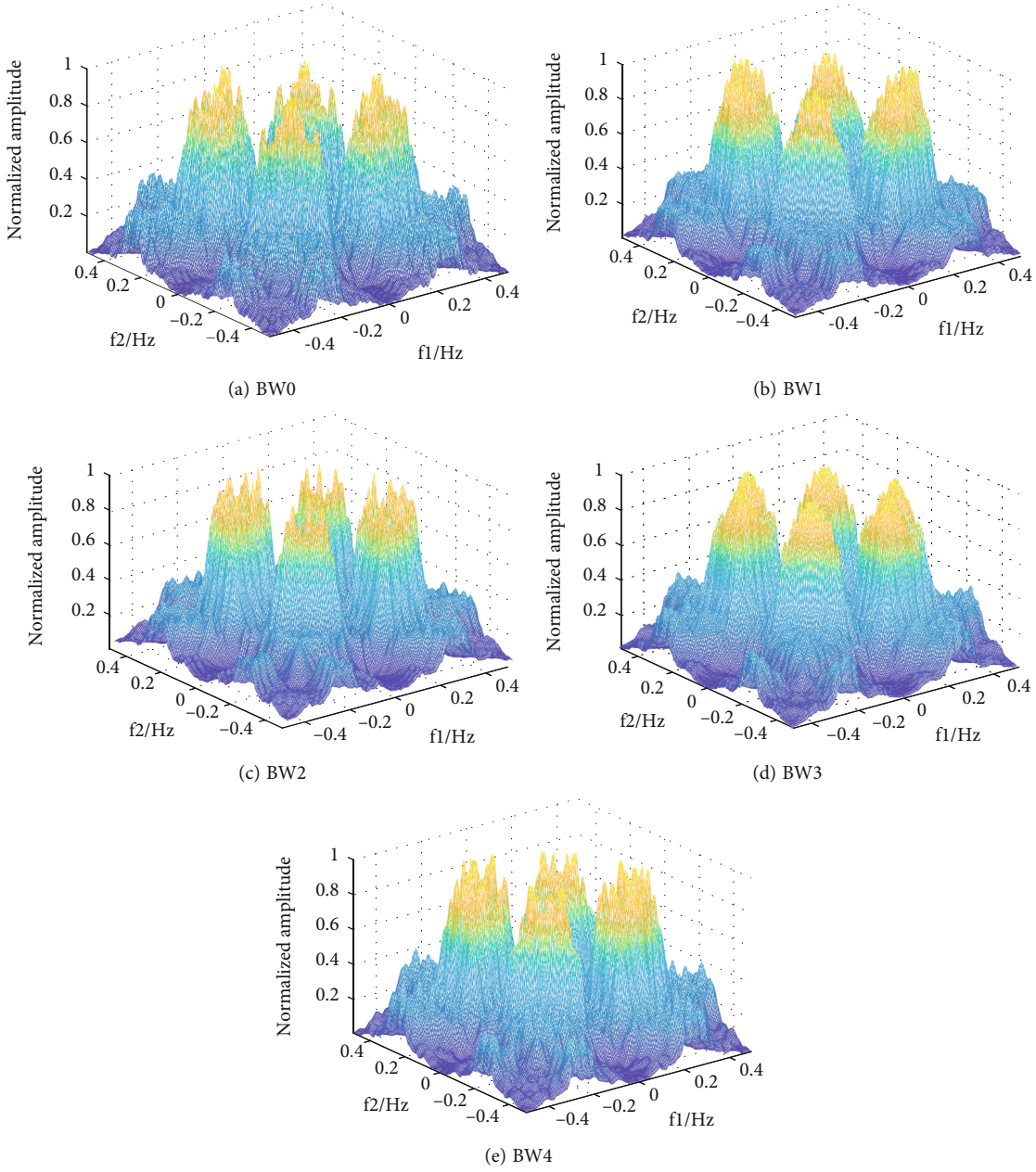

Figure 7: Autocorrelation spectrogram (SNR = 0 dB).

For the convenience of observation, in Figure 8(a), we draw the contour map of Figure 7(a). The contour map can be considered as a two-dimensional representation of the three-dimensional autocorrelation spectrogram image. As a comparison, we also draw the autocorrelation spectrogram contour map of BW0 when the SNR is 5 dB, as shown in Figure 8(b).

According to Figure 8, we know that when the SNR is 0 dB, the autocorrelation spectrogram contour map is cluttered due to the influence of noise. When the SNR increases to 5 dB, the noise part is basically invisible, which proves the effectiveness of the autocorrelation method we select in denoising. It is feasible to extract the autocorrelation spectrogram features of the signal.

The process of extracting features is shown in Table 2.

3.4. Neural Network Model. In this section, we design a two-input CNN. Compared with the traditional CNN, two independent inputs represent two different network models, which can further learn the extracted features, which further reduces the probability of misclassification. The network model we designed can be considered to have two independent model structures because of its two branches. These two independent models only have convolutional layers, pooling layers, and fully connected layers, which are simple in structure, easy to implement, and fast to compute. Figure 9 is the framework of the two-input CNN we designed, which shows the basic structure of the network in this paper.

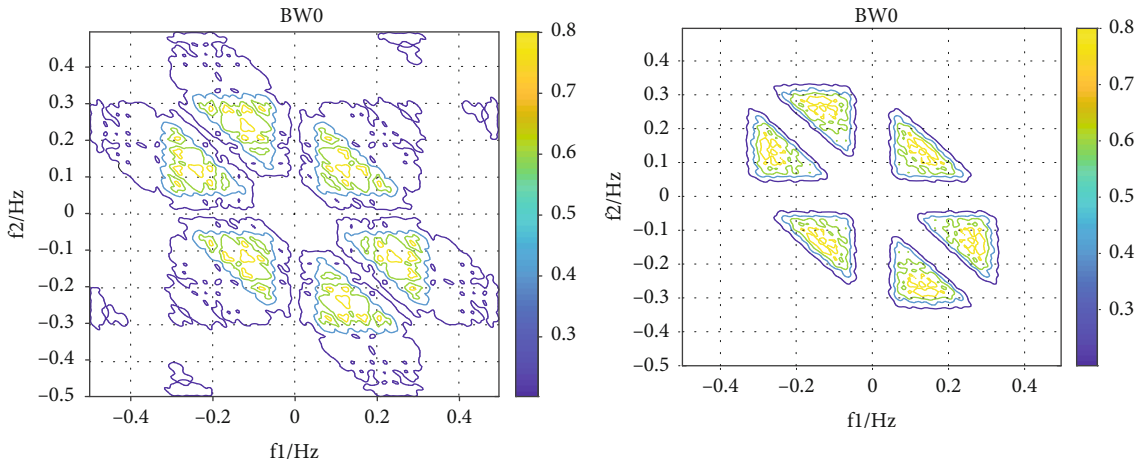

(a) BW0, SNR = 0 dB (b) BW0, SNR = 5 dB

Figure 8: Contour maps of autocorrelation spectrogram.

Table 2: The process of extracting autocorrelation spectrogram features.

Step	Detailed process
Step 1	signal generation: According to the MIL-STD-188-141B standard, generate five types of burst waveforms with noise
Step 2	calculate the autocorrelation function: Based on Equation (5), calculate the autocorrelation function R_{ss}, to achieve the purpose of noise reduction
Step 3	bispectrum transformation: According to Equation (6) and (7), calculate the bispectrum transformation matrix S_{3s} of R_{ss}. The dimension of S_{3s} is 256×256
Step 4	down sampling: For matrix S_{3s}, sample one sample point for every two points, so that the matrix dimension becomes 256×128, to realize the dimension reduction of the matrix
Step 5	constructing a three-dimensional matrix: Extract the odd and even rows of the matrix, respectively, and construct matrices S_{3s1} and S_{3s2} with a dimension of 128×128. S_{3s1} and S_{3s2} are the first and second channels of the three-dimensional matrix M, and the dimension of M becomes $128 \times 128 \times 2$
	M is the extracted feature matrix

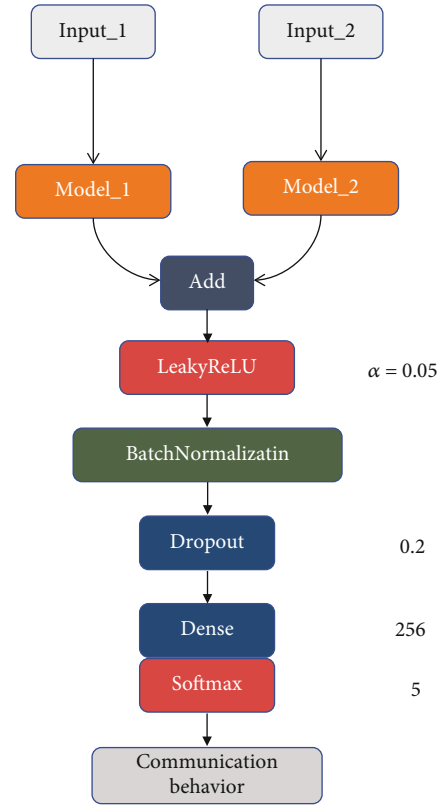

Figure 9: Network framework.

The extracted features are subjected to convolution operations in the two models, and then two outputs are obtained. The two outputs are merged through the add layer, and then through the subsequent layers, the classification task can be completed.

Figure 10 shows the specific structure of the two branches Model 1 and Model 2. Among them, the first branch has a small number of layers, only two convolution layers and two fully connected layers. After convolution calculation, features can be learned quickly and effectively. The second branch has more convolutional and fully connected layers than the first branch. The operation time of this branch is longer, but further features can be learned. Compared with traditional CNN, the model has stronger learning ability by using two branches to learn features separately. At the same time, because the number of layers in the first branch is relatively small, the extra calculation time consumption brought by the design of the two inputs is not much.

In this paper, the inputs of both two branches are autocorrelation spectrogram feature matrix M extracted in Table 2.

The training process of our neural networks is summarized in Table 3.

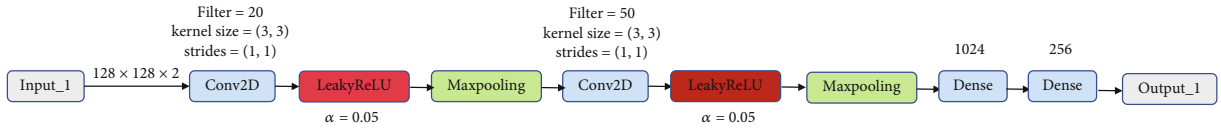

(a) Model 1

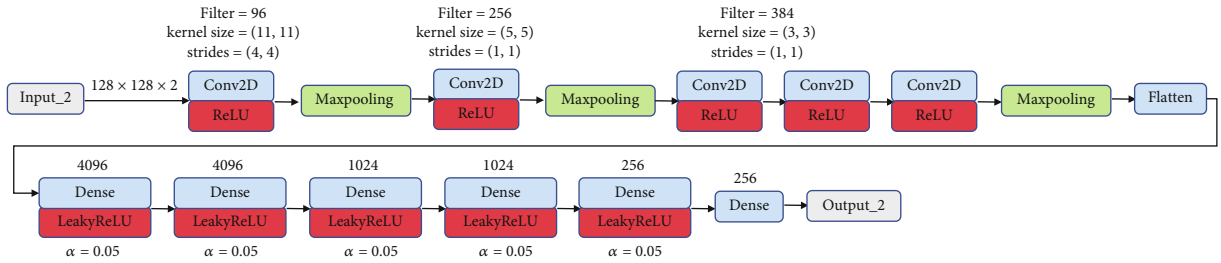

(b) Model 2

Figure 10: Network model.

Table 3: Training process.

Step	Training process
Step1	send the feature matrix M obtained by Table 2 to the two inputs of the network
Step2	convolutional calculations, obtain two outputs X_1 and X_2, both of them have 256 dimensions
Step3	consider X_1 and X_2 as two new inputs, and through the add layer, X is obtained, $X = X_1 + X_2$
Step4	let X pass through the last few layers, the communication behavior identification is completed

4. Experiments

The experiments consist of the following parts. First, the recognition accuracy of the proposed algorithm for five communication behaviors is compared under different SNR conditions, meanwhile, the effects of different parameters on the experimental results are compared. Then, the improvement in the results of our proposed algorithm is verified by comparison with the previous algorithm. Finally, the recognition results of different network models are compared.

The experimental parameters are set as follows: 5000 samples are selected. The number of training sets and test sets is divided into 4 to 1, and 25% of the training sets are randomly selected as validation sets. We use the momentum optimizer, which dynamically adjusts the learning rate. The initial learning rate of the network is 0.01; the attenuation factor of the learning rate is 1e-6; the batch size is 64, and the epoch is 500.

Experimental Environment: Windows 10 Operating System, 11th Gen Intel (R) Core (TM) I5-11260H CPU, NVIDIA GeForce RTX3050, Python 3.7, TensorFlow 2.5.0, and Keras 2.8.0.

4.1. Verify the Validity of the Algorithm. According to the experimental parameters, the algorithm should first be verified. When the SNR is 0 dB, 5 dB, 8 dB, 10 dB, and 15 dB, respectively; the recognition results on the test set are shown in Figure 11. The results illustrate that BW1 and BW2 are most easily classified into wrong classes. When the SNR is not lower than 5 dB, the recognition accuracy of each communication behavior can reach more than 80%, and with the reduction of noise, the recognition accuracy can reach close to 100%.

Figures 12–14 show the comparison of different initial learning rates, different attenuation factors, and different batch sizes, respectively.

The experimental results show that when the initial learning rate is 0.01, and the attenuation factor is 1e-6; the learning ability of our designed network is the best. When the batch size is 64, 32 and 16, the learning ability of the network is not much different. However, according to Table 4, when the batch size is 64, the learning time per epoch is the shortest. As a result, it is reasonable to set the batch size to 64.

4.2. Experimental Comparison of Different Algorithms. Currently, the research on radio behavior recognition based on signals from the physical layer is in its infancy, and only the study in [33] carries out communication behavior recognition based on five types of burst waveforms. When the SNR is 15 dB, the recognition accuracy can reach 99.3%, but with the increase in noise, the recognition accuracy obviously decreases. When the SNR is lower than 8 dB, the overall recognition accuracy is lower than 80%. When the SNR is 0 dB, it is even lower than 50%. In this experiment, we compare the algorithm proposed in this paper with the algorithm in the literature [33] as well as the network model in this paper plus, the features in the literature [33], and the network model in this paper plus the features in the literature [33]. The experimental results are illustrated in Figure 15.

It can be observed that the algorithm proposed in this letter offers the best results, especially on the lower SNR

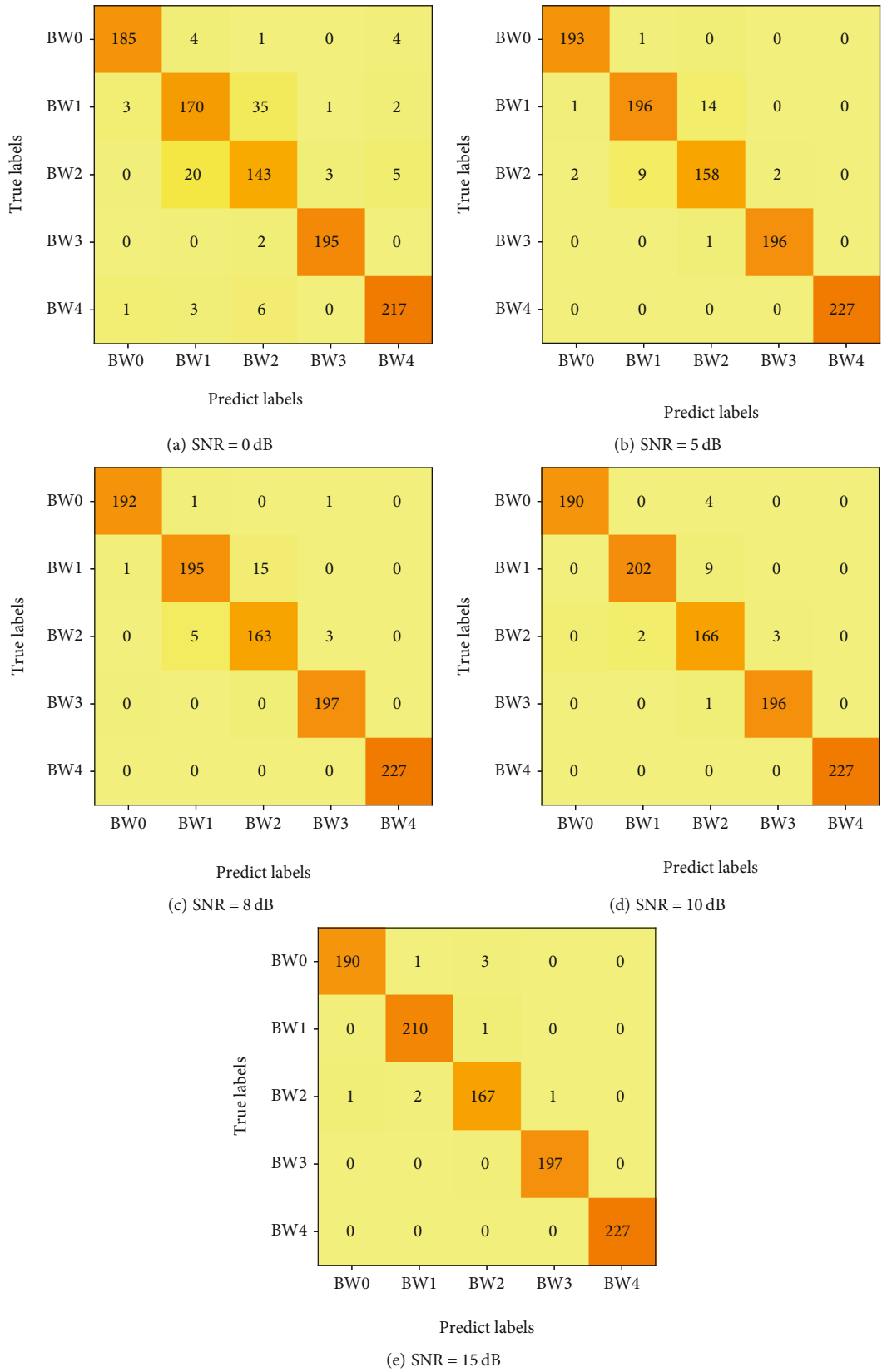

(a) SNR = 0 dB

(b) SNR = 5 dB

(c) SNR = 8 dB

(d) SNR = 10 dB

(e) SNR = 15 dB

Figure 11: Confusion matrices for five communication behaviors.

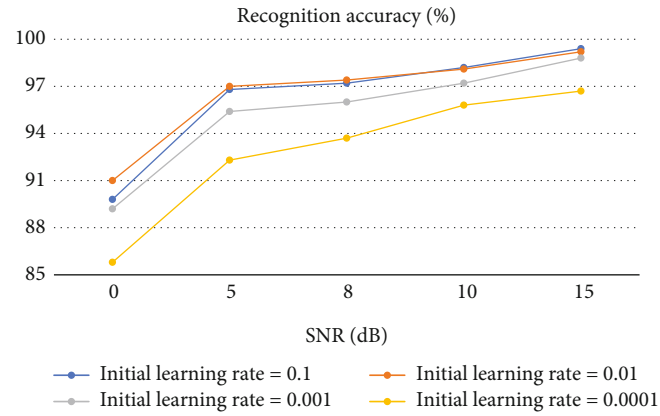

Figure 12: Comparative experiments with different initial learning rates.

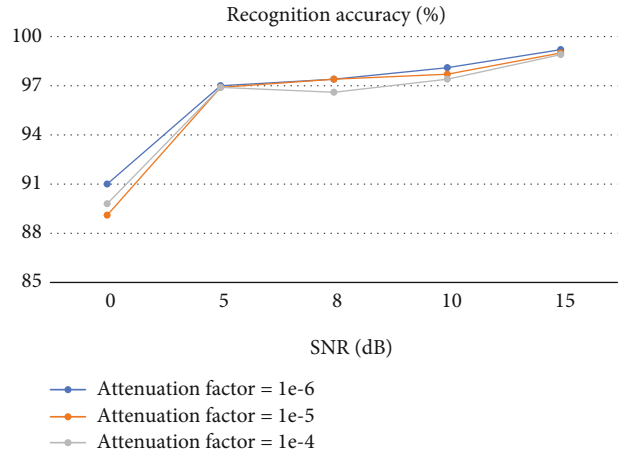

Figure 13: Comparative experiments with different attenuation factors.

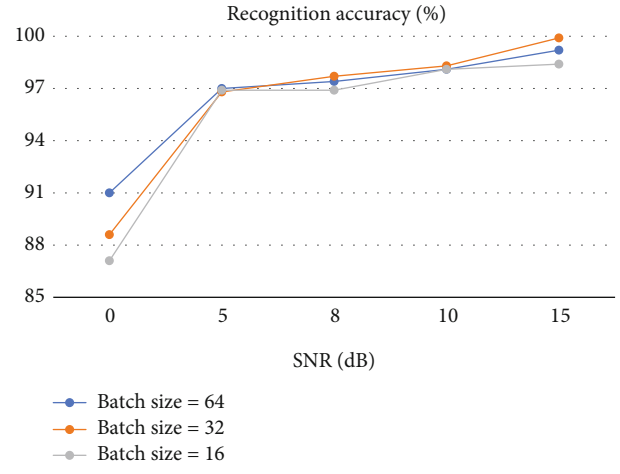

Figure 14: Comparative experiments with different batch sizes.

conditions. Since the autocorrelation denoising method can effectively eliminate noise; our algorithm can significantly improve recognition accuracy. Even if the SNR is 0 dB, the accuracy can still reach 91%. When the SNR is 5 dB, 8 dB, and 10 dB, the accuracy of the algorithm in this letter can increase by 23.8%, 15.9%, and 3.6%, respectively, compared to the algorithm in literature [33]. When the SNR is 15 dB, the influence of noise can be ignored, and the autocorrelation method to reduce noise will cause the loss of information from the original signals, which results in the loss of features. This part of the loss offsets the influence of noise, making the accuracy slightly lower than in the literature [33], but it can still reach 99.2%.

Table 4: Training time for a single epoch.

Batch size	Time(s)
64	4.079
32	5.055
16	8.044

If we extract the autocorrelation spectrogram features and select the network model in the literature [33], the recognition accuracy under low SNR conditions can still be effectively improved. When the SNR is 0 dB, 5 dB, 8 dB, and 10 dB, the recognition accuracy can increase by 43.6%,23.0%, 15.9%, and 3.4%, respectively. When the SNR is 15 dB, due to the loss of features caused by the denoising method, the recognition accuracy is lower than that of literature [33]. Compared with the method in this paper, the recognition accuracy is also lower due to the simple network.

In addition, when the extracted features are autocorrelation spectrogram features, the recognition accuracy can be further improved by using the network in this paper.

4.3. Comparison of Different Network Models. This experiment compares the recognition accuracy of several classical convolutional neural networks. First, as representatives of simple convolutional neural networks, AlexNet and LeNet are chosen as comparison objects. Classic network models such as VGG-19 and ResNet34 are also compared. When the network tends to be stable, the experimental results of different network models are shown in Figure 16.

AlexNet itself is easy to implement due to its simple structure, and its experimental results are better than those of LeNet and VGG-19, and slightly inferior to ResNet34.

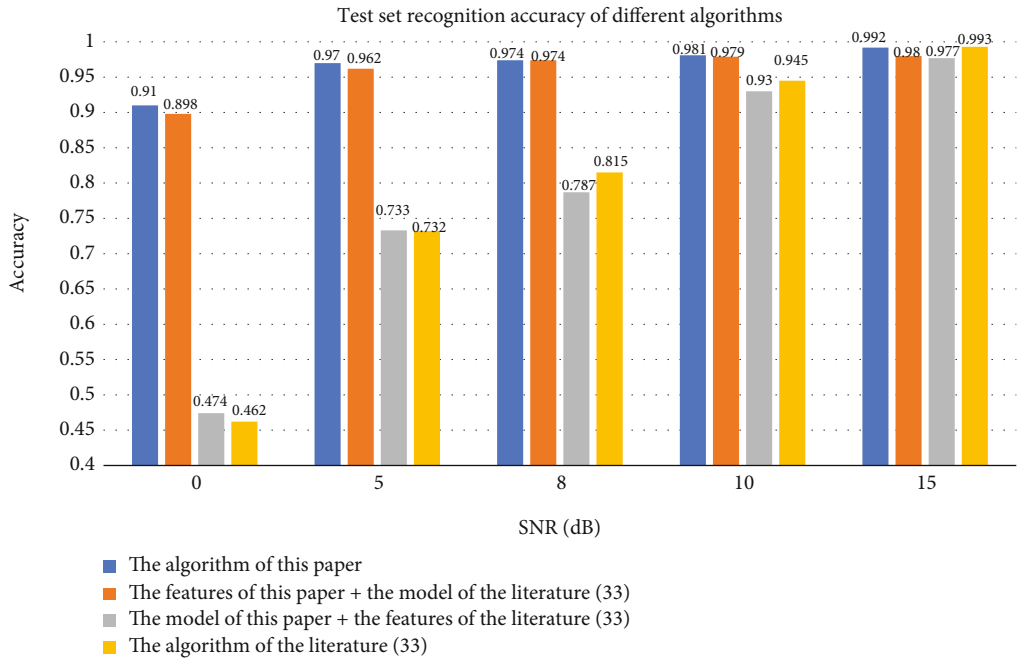

Figure 15: Comparison of different algorithms.

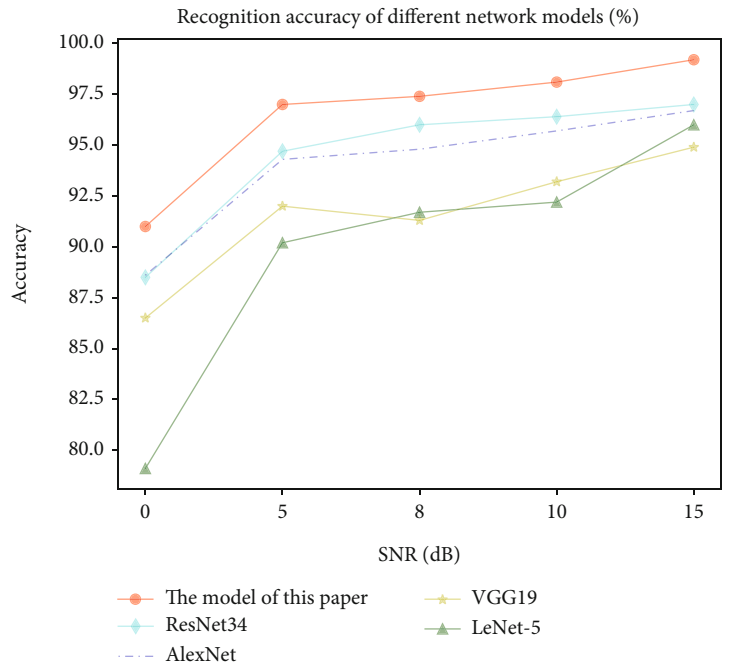

Figure 16: Recognition results of different network models.

When the SNR ranges from 0 to 15 dB, our network model can perform better recognition, which is superior to traditional CNNs.

5. Conclusions

In this paper, we carry out research on the identification of shortwave radio communication behavior, starting from five types of burst waveforms in the physical layer. A signal feature extraction method based on autocorrelation spectrogram features is proposed. A neural network model is improved to further optimize the algorithm. The experimental results prove that the autocorrelation spectrogram features are not easily affected by noise, and the proposed network can further improve the recognition results. Our proposed algorithm can dramatically improve recognition results under low SNR conditions. Behavioral learning is increasingly important in communications, as a typical CRS, shortwave radio is just the first research object in a series of relevant works. Our subsequent work will continue

to focus on behavior recognition research on the CRS. In the future, we aim to expand related research to more types of CRS and wider communication scenarios, and consider more environmental factors, which is quite meaningful for communication confrontation.

Data Availability

Each burst waveform is generated according to the third-generation shortwave communication protocol standard. The dataset we use is made according to the feature extraction process mentioned in this paper. You can also ask for the data by contacting lihaitao_01@163.com.

Conflicts of Interest

The authors declare that they have no conflicts of interest.

Acknowledgments

We would like to thank the National Natural Science Foundation of China, for the research on several key technologies for the individual identification of communication radiation sources in complex electromagnetic environments. (Grant 62071479).

References

[1] I. Lee, D. Kim, and S. Lee, "3-D human behavior understanding using generalized TS-LSTM networks," *IEEE Transactions on Multimedia*, vol. 23, pp. 415–428, 2021.

[2] Z. Zhigang, D. Guangxue, L. Huan, Z. Guangbing, W. Nan, and Y. Wenjie, "Human behavior recognition method based on double-branch deep convolution neural network," in *2018 Chinese Control And Decision Conference (CCDC)*, pp. 5520–5524, Shenyang, China, 2018.

[3] Z. Shi, L. Cao, Y. Han, H. Liu, F. Jiang, and Y. Ren, "Research on recognition of motion behaviors of copepods," *IEEE Access*, vol. 8, pp. 141224–141233, 2020.

[4] S. Mukhopadhyay and H. Leung, "Recognizing human behavior through nonlinear dynamics and syntactic learning," in *Conference Proceedings - IEEE International Conference on Systems, Man and Cybernetics*, pp. 846–850, Seoul, Korea, 2012.

[5] H.-L. Chen, M. J. Tsai, and C. C. Chan, "A hidden Markov model-based approach for recognizing swimmer's behaviors in swimming pool," in *2010 International Conference on Machine Learning and Cybernetics*, pp. 2459–2465, Qingdao, China, 2010.

[6] Z. Jiang, D. Crookes, B. D. Green et al., "Context-aware mouse behavior recognition using hidden Markov models," *IEEE Transactions on Image Processing*, vol. 28, no. 3, pp. 1133–1148, 2019.

[7] M. Quaid and A. Jalal, "Wearable sensors based human behavioral pattern recognition using statistical features and reweighted genetic algorithm," *Multimedia Tools and Applications*, vol. 79, no. 9-10, pp. 6061–6083, 2020.

[8] K. Wu, H. Jiang, and C. Tellambura, "Cooperative sensing with heterogeneous spectrum availability in cognitive radio," *IEEE Transactions on Cognitive Communications and Networking*, vol. 8, no. 1, pp. 31–46, 2022.

[9] M. Alaee-Kerahroodi, E. Raei, S. Kumar, and M. Bhavani Shankar, "Cognitive radar waveform design and prototype for coexistence with communications," *IEEE Sensors Journal*, vol. 22, no. 10, pp. 9787–9802, 2022.

[10] W. Lu, P. Si, G. Huang, H. Han, and L. Qian, "SWIPT cooperation spectrum sharing for 6G-enabled cognitive IoT network," *IEEE Internet of Things Journal*, vol. 8, no. 20, pp. 15070–15080, 2020.

[11] H. Li, Y. Li, C. He, J. Zhan, and H. Zhang, "Cognitive electronic jamming decision-making method based on improved-learning algorithm," *International Journal of Aerospace Engineering*, vol. 2021, Article ID 8647386, 12 pages, 2021.

[12] A. Darpa, "Behavioral learning for adaptive electronic warfare," in *Darpa-BAA-10-79, Defense Advanced Research Projects Agency*, Arlington, USA, 2010.

[13] Y. Wu, X. Li, and J. Fang, "A deep learning approach for modulation recognition via exploiting temporal correlations," in *2018 IEEE 19th International Workshop on Signal Processing Advances in Wireless Communications (SPAWC)*, pp. 1–5, Kalamata, Greece, 2018.

[14] G. Liu and J. Cao, "Research on modulation recognition of OFDM signal based on hierarchical iterative support vector machine," in *2020 International Conference on Communications, Information System and Computer Engineering (CISCE)*, pp. 38–44, Kuala Lumpur, Malaysia, 2020.

[15] S. Ansari, K. A. Alnajjar, S. Abdallah, and M. Saad, "Automatic digital modulation recognition based on machine learning algorithms," in *2020 International Conference on Communications, Computing, Cybersecurity, and Informatics (CCCI)*, pp. 1–6, Sharjah, United Arab Emirates, 2020.

[16] F. Liu, Z. Zhang, and R. Zhou, "Automatic modulation recognition based on CNN and GRU," *Tsinghua Science and Technology*, vol. 27, no. 2, pp. 422–431, 2022.

[17] X. Li and Y. Lei, "Radiation source individual identification using machine learning method," in *2019 IEEE 8th Joint International Information Technology and Artificial Intelligence Conference (ITAIC)*, pp. 1001–1005, Chongqing, China, 2019.

[18] Y. Chen, L. Yu, Y. Yao, and L. Zhu, "Individual identification technology of communication radiation sources based on deep learning," in *2020 IEEE 20th International Conference on Communication Technology (ICCT)*, pp. 1301–1305, Nanning, China, 2020.

[19] L. Ying, J. Li, and B. Zhang, "Differential complex-valued convolutional neural network-based individual recognition of communication radiation sources," *IEEE Access*, vol. 9, pp. 132533–132540, 2021.

[20] S. Yang, H. Peng, M. Xu, Y. Pan, and X. Hou, "Ultra-shortwave specific signal spectrogram recognition based on convolution neural network," *Journal of Systems Engineering and Electronics*, vol. 47, no. 4, pp. 744–751, 2019.

[21] X. Cha, M. Xu, H. Peng, X. Qin, and T. Li, "Specific protocol signal recognition based on deep residual network," *Acta Electronica Sinica*, vol. 47, no. 7, pp. 1532–1537, 2019.

[22] Q. Jin, X. Gou, W. Jin, and N. Wu, "Intention recognition of aerial targets based on Bayesian optimization algorithm," in *2017 2nd IEEE International Conference on Intelligent Transportation Engineering (ICITE)*, pp. 356–359, Singapore, Singapore, 2017.

[23] X. Gou and N. Wu, "Air group situation recognition method based on GRU-attention neural network," *Computer and Modernization*, vol. 35, no. 10, pp. 11–16, 2019.

[24] C. Liu, X. Wu, C. Yao, L. Zhu, Y. Zhou, and H. Zhang, "Discovery and research of communication relation based on communication rules of ultrashort wave radio station," in *2019 IEEE 4th International Conference on Big Data Analytics (ICBDA)*, pp. 112–117, Suzhou, China, 2019.

[25] C. Liu, X. Wu, L. Zhu et al., "The communication relationship discovery based on the spectrum monitoring data by improved DBSCAN," *IEEE Access*, vol. 7, pp. 121793–121804, 2019.

[26] C. Liu, X. Wu, L. Zhu et al., "Research on communication network structure mining based on spectrum monitoring data," *IEEE Access*, vol. 8, pp. 3945–3959, 2020.

[27] C. Liu, X. Wu, C. Yao et al., "Research on discovery of radio communication relationship based on correlation analysis," *IOP Conference Series: Earth and Environmental Science*, vol. 440, no. 4, article 042006, 2020.

[28] T. Pan, X. Wu, C. Yao, Y. Zhou, and X. Lu, "Communication behavior structure mining based on electromagnetic spectrum analysis," in *2019 IEEE 8th Joint International Information Technology and Artificial Intelligence Conference (ITAIC)*, pp. 1611–1616, Chongqing, China, 2019.

[29] K. Cheng, L. Zhu, C. Yao et al., "DCGAN based spectrum sensing data enhancement for behavior recognition in self-organized communication network," *China Communications*, vol. 18, no. 11, pp. 182–196, 2021.

[30] J. Zhang, M. Tan, F. Shi, Y. Yang, and Z. Yang, "A novel approach of protocol behavior identification for TDMA-based frequency hopping communication," *Wireless Communication and Mobile Computing*, vol. 2022, article 7941367, pp. 1–14, 2022.

[31] X. You and W. Ge, "Protocol identification and multi-conversation relationship extraction in Fetion," *Modern Electronics Technique*, vol. 37, no. 21, pp. 19–23, 2014.

[32] H. Zhou, L. Yang, and Z. Wu, "Feasibility analysis of tactical radio station communication behaviors cognition," in *2021 Asia-Pacific Conference on Communications Technology and Computer Science (ACCTCS)*, pp. 160–166, Shenyang, China, 2021.

[33] Z. Wu, H. Chen, and Y. Lei, "Recognizing non-collaborative radio station communication behaviors using an ameliorated LeNet," *Sensors*, vol. 20, no. 15, pp. 1–20, 2020.

[34] Z. Wu, H. Chen, Y. Lei, and H. Xiong, "Recognizing automatic link establishment behaviors of a short-wave radio station by an improved unidimensional DenseNet," *IEEE Access*, vol. 8, pp. 96055–96064, 2020.

[35] Z. Wu, H. Chen, and Y. Lei, "Visualization research on improved DenseNet applied to recognize a radio station's link establishment behavior," *Journal of Systems Engineering and Electronics*, vol. 43, no. 5, pp. 1371–1381, 2021.

[36] Z. Wu, H. Chen, and Y. Lei, "Unidimensional ACGAN applied to link establishment behaviors recognition of a short-wave radio station," *Sensors*, vol. 20, no. 4270, pp. 1–19, 2020.

[37] Y. Xie and H. Deng, "A radio frequency fingerprinting identification method based on improved ResNet," *Telecommunication Engineering*, vol. 62, no. 4, pp. 416–423, 2022.

[38] J. Jia and L. Qi, "RF fingerprint extraction method based on bispectrum," *Journal of Terahertz Science and Electronic Information Technology*, vol. 19, no. 1, pp. 107–111, 2021.